SUPERGRANULATION ROTATION

John G. Beck and Jesper Schou
W.W. Hansen Experimental Physics Laboratory
Stanford, CA 94305-4085.

December 11, 1999

Abstract. Simple convection models estimate the depth of supergranulation at approximately 7,500 km which suggests that supergranules would rotate at the rate of the plasma in the outer 1% of the solar radius. The supergranulation rotation obtained from MDI dopplergrams shows that supergranules rotate faster than the outer 5% of the convection zone and show zonal flows matching results from inversions of f-mode splittings. Additionally, the rotation rate depends on the size scale of the features.

Keywords: rotation, supergranulation

1. Introduction

While studying solar rotation, Hart (1954) found a photospheric velocity field with an amplitude of 170 $\mathrm{m\,s^{-1}}$ persisting for several hours. Upon further study, a size scale of 26,000 km was determined (Hart, 1956). Leighton, Noyes and Simon (1962) confirmed the existence of these features, finding cells with diameters of 30,000 km, rms velocities of 500 $\mathrm{m\,s^{-1}}$ and lifetimes of 10^4 to 10^5 seconds. They called this phenomenon 'supergranulation' and attributed it to convection.

Subsequently, Simon and Leighton (1964) measured a mean supergranulation lifetime of 20 hours and reported a strong spatial correspondence of supergranule cells boundaries with the magnetic network. Since the cells were irregularly shaped and had a large horizontal extent in comparison to the lifetime and vertical velocity, Simon and Leighton suggested that supergranulation appeared to be non-stationary convection. They used the relation that the cell depth is approximately equal to the product of the vertical velocity and the lifetime to obtain a depth estimate of 7,200 km. Additionally, Duvall (1998) applied the technique of time-distance helioseismology to the study of supergranules and found evidence suggesting that supergranules have a depth of 8,000 km.

The geometry of supergranules suggests they are convective cells. Supergranules are horizontal outflows from regions of up-welling at their center to sinks at their boundaries. However, if supergranules transport heat, the temperature at their centers should be higher than at their boundaries. Several studies have attempted to detect a temperature

contrast (eg. Simon and Leighton, 1964; Beckers, 1968; Worden, 1975; and Foukal and Fowler, 1984) but the results have been inconclusive. Lin and Kuhn (1992) established an upper limit of the temperature contrast of 3K. Using time-distance helioseismology, Duvall *et al.* (1997) mapped out three dimensional structures of supergranules and found the heat flow was inconsistent with convection. Supergranules are not the only features suspected of being large scale convection. The giant cells detected by Beck, Duvall and Scherrer (1998) are another large-scale velocity pattern which show hints but no direct evidence of being convective in origin.

2. Data Reduction and Analysis

We used full-disk dopplergrams obtained from the MDI instrument during the period from 24 May 1996 to 22 July 1996. The data were filtered using a tapered Gaussian filter with a FWHM of 8 minutes and a window width of 31 minutes (Hathaway, 1988), which reduced the p-mode signal to about 1 $\mathrm{m\,s^{-1}}$. Solar rotation introduces an east-west blurring into averaged dopplergrams; this was remedied by resampling the images to remove the east-west shift due to rotation before averaging. The de-rotated, temporally-filtered dopplergrams were produced with 15-minute sampling.

The averaged images were first apodized with a cosine between 0.90R and 0.95R, where R is the radius of the solar image, in order to reduce edge effects. Given the nature of the following analysis this form of apodization is not ideal, though it works well at moderate latitudes. Next the images were remapped to a uniform grid in longitude ϕ and sin(latitude), creating a data cube. In a cut at constant latitude supergranules appear to be moving along diagonal lines with a slope given by the rotation rate Ω at that latitude. Rather than trying to measure this slope directly the data cube was Fourier transformed in longitude and time yielding a (sin(latitude), m, ν) power spectrum. This method produces similar results as cross-correlating each size scale separately. Cuts through a spectrum are shown in Figures 1, 2 and 3. It may be shown (forgetting about projection effects and the fact that not all longitudes can be observed) that a feature with a velocity pattern proportional to $\cos(m\phi + \phi_0)$ rotating at a rate Ω will show up at a frequency ν given by $2\pi\nu = \omega = m\Omega$ allowing the determination of Ω as a function of latitude and m.

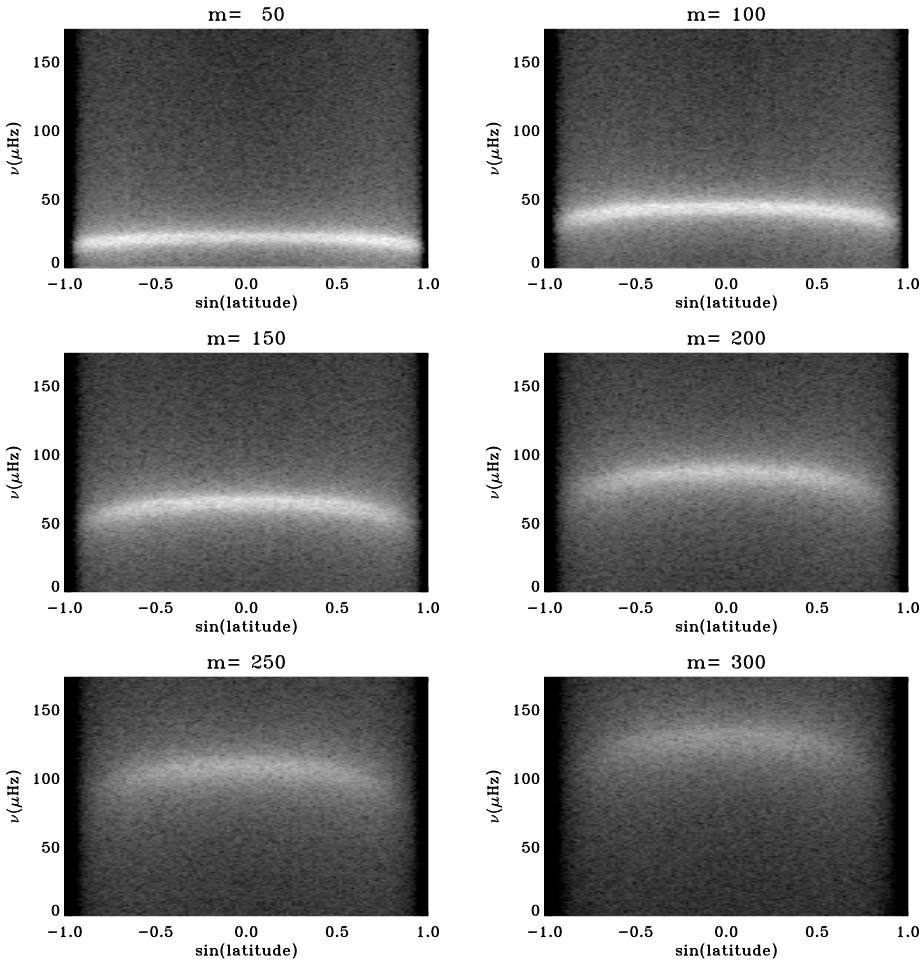

Figure 1. The power spectrum as a function of sin(latitude) and ν for various m values. The power is shown using a log scale. The differential rotation can be seen as the curve of the ridge.

3. Results

3.1. Rotation Measurements

To determine the rotation rate of supergranules, the location of the peaks in the power spectrum were measured by their center of gravity calculated over a symmetric interval of $\approx 58\,\mu$Hz around an initial guess (which is then iterated). For the lowest m's the interval was reduced symmetrically using only positive frequencies since the zero frequency point contained large artifacts due to calibration errors.

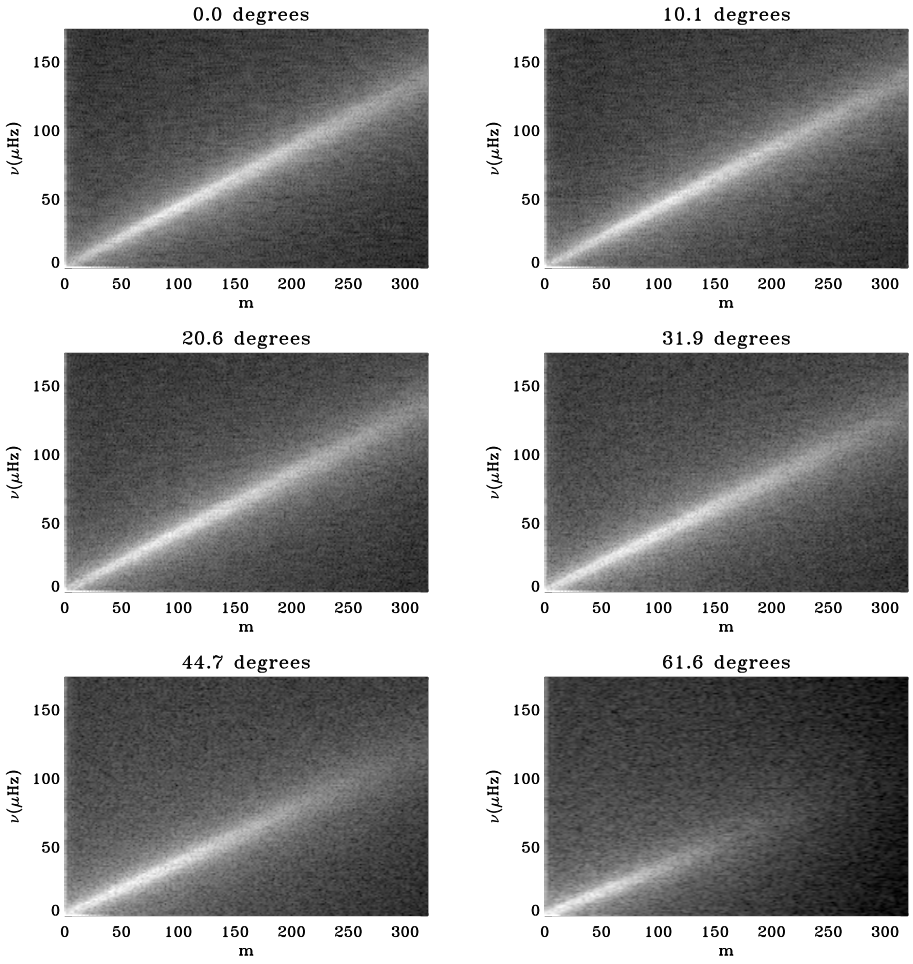

Figure 2. The power spectrum as a function of sin(latitude) and ν for various latitudes. Otherwise like Fig. 1.

For the results shown here power spectra for six 10 day intervals, covering the period 24 May 1996 through 22 July 1996, were averaged before measuring the peak positions and the corresponding rotation rates.

Figures 1, 2 and 3 show various cuts through the power spectrum to illustrate the basic idea behind the method. Notice in particular that the signal to noise ratio for the peaks is quite high and that the differential rotation is easily visible in Figure 1.

Figure 4 shows the inferred rotation near the equator as a function of m. The downturn in the rotation rate at $m < 20$ is most likely an artifact of the peak being very close to zero frequency making it hard

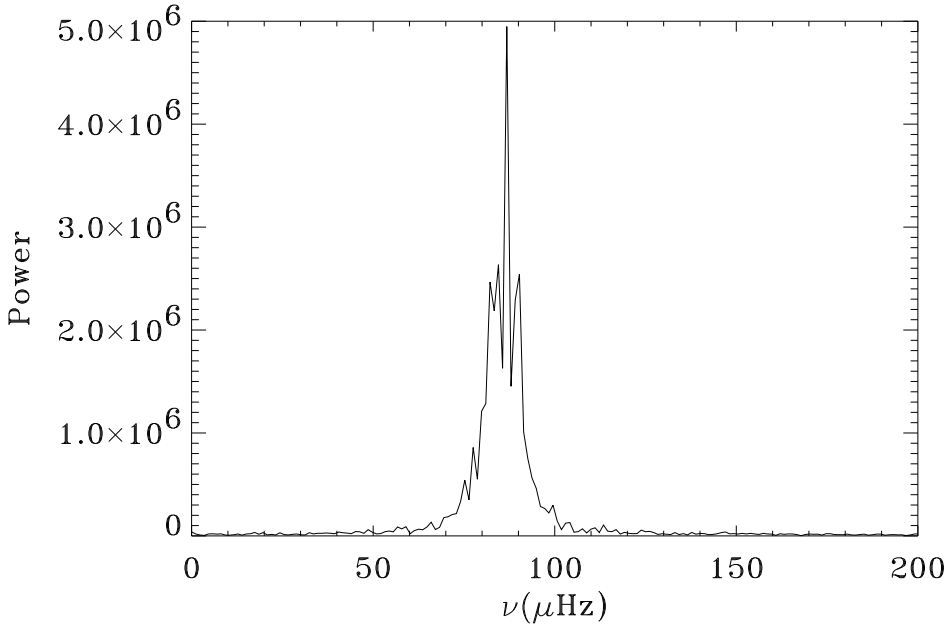

Figure 3. The power as a function of ν for the equator and $m = 200$.

to measure accurately due to the difficulty in tracking large features over a fraction of a rotation.

Figure 5 shows the rotation rates at various m values as a function of latitude together with various rotation rates from the literature.

3.2. Comparisons With Inversions results

To search for zonal flows, a second order polynomial in $\sin^2$(latitude) was subtracted from an average supergranulation rotation curve, producing the residuals shown in Figure 6. Figure 7 shows the symmetric component of the residuals and compares the results with those from an analysis of f-mode splittings (Schou, 1999) which were obtained from data from roughly the same period as the data for the present analysis.

Figures 8 and 9 compare supergranulation rotation rates with the results of an RLS rotation inversion, from Schou *et al.* (1998). Noting that the supergranulation power spectrum produced by Hathaway *et al.* 1996 showed a broad peak around $m = 70$, we averaged the rotation rates over the range: $50 \leq m \leq 100$. This was compared with the measurement of Snodgrass and Ulrich (1990) and the rotation rates at various depths within the outer 10% of the convection zone.

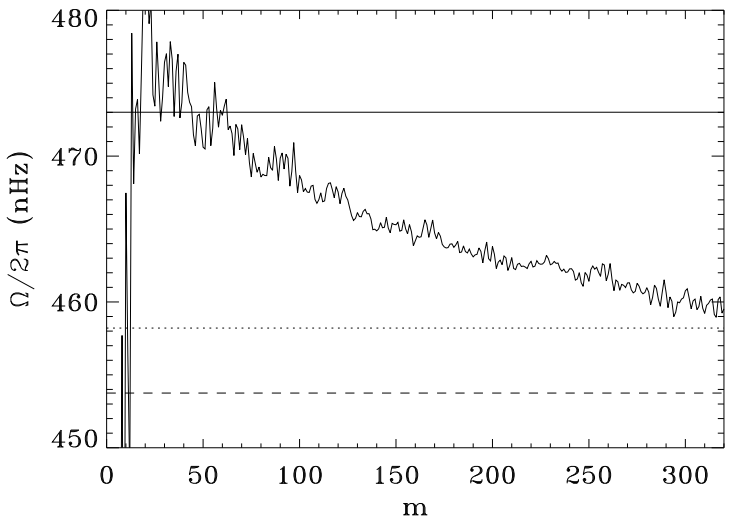

Figure 4. The inferred rotation rate as a function of m. The results were averaged over $\pm 9^\circ$ around the equator. Also shown are various surface rotation rates. The horizontal lines are rotation rates from Snodgrass and Ulrich (1990); the solid line is the supergranulation rate, the dotted line is the rate of magnetic tracers and the dashed line is the spectroscopic rate.

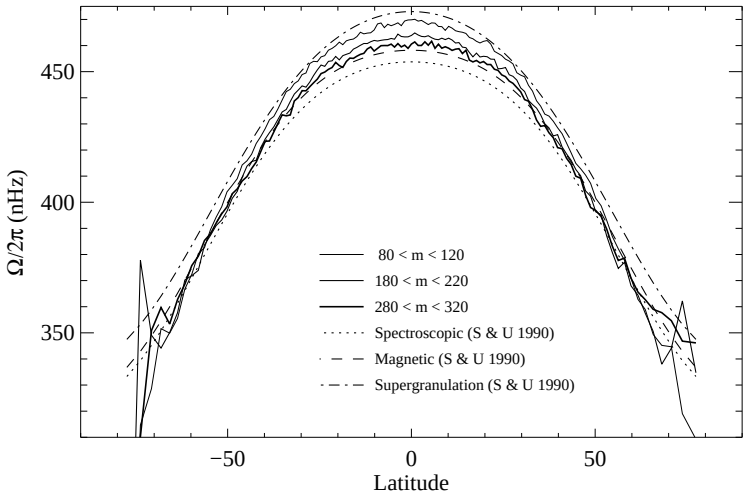

Figure 5. The inferred rotation rates as a function of latitude for various m ranges.

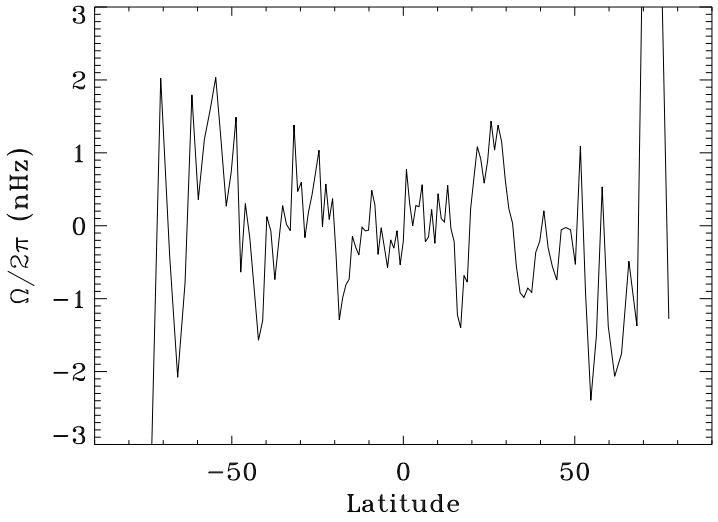

Figure 6. The rotation rate, averaged over $80 \leq m \leq 320$, as a function of latitude after subtraction of a fit of a second order polynomial in $\sin(\text{latitude})^2$.

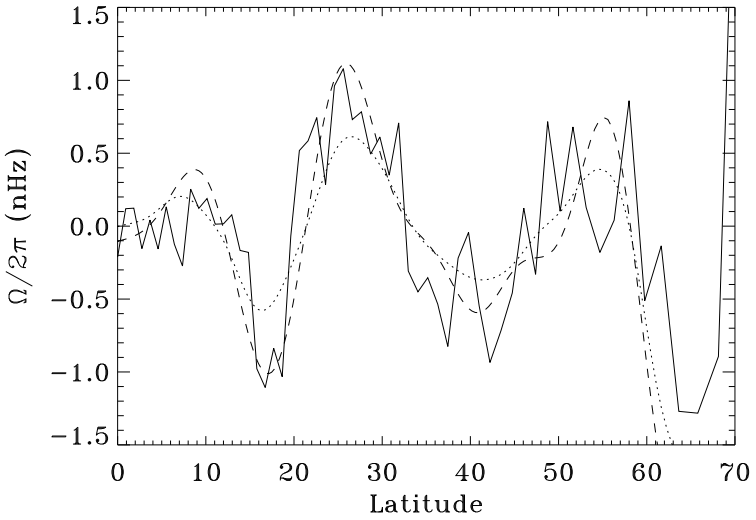

Figure 7. The symmetric component of the results shown in Fig. 6 (solid line). Also shown are the results from analyzing f mode splittings (Schou, 1999), also after subtraction of a second order polynomial in $\sin(\text{latitude})^2$. The dotted line is a MOLA inversion while the dashed line is a RLS inversion.

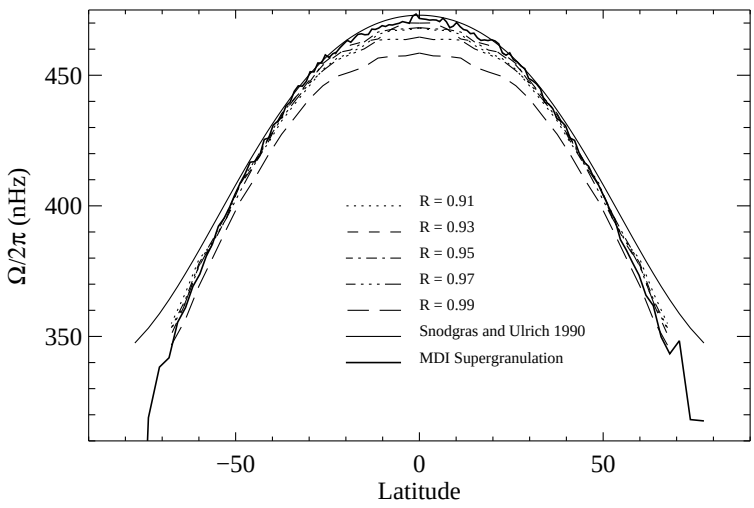

Figure 8. Supergranule Rotation rates averaged over $50 \leq m \leq 100$ compared with rotation rates obtained for various depths within the convection zone, from Schou *et al.* (1998) and Snodgrass and Ulrich (1990) supergranulation rotation measurement

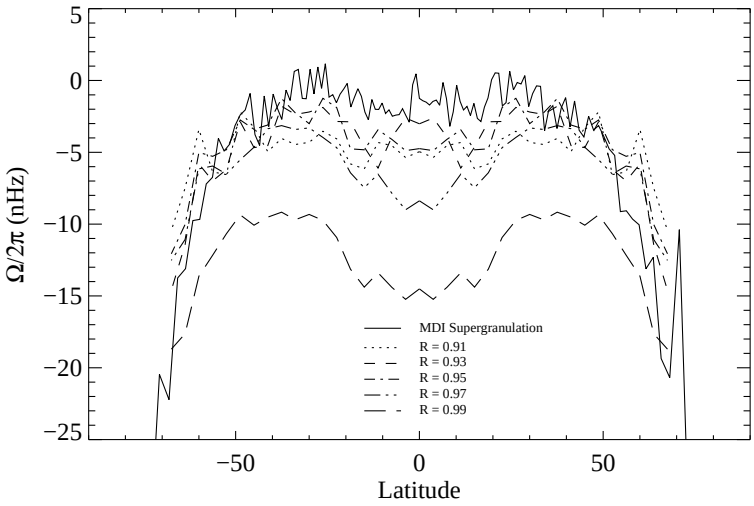

Figure 9. This plot shows the curves from Figure 8 with the Snodgrass and Ulrich (1990) supergranulation rotation curve subtracted.

Figure 8 shows the rotation curves of the supergranulation size scales, the Snodgrass and Ulrich (1990) supergranulation rotation measurement and the RLS rotation rates at five depths within the outer 10% of the convection zone. The depth of maximum rotation rate is 0.93 $R_\odot$, having a rate of 470 nHz at the equator. The MDI supergranule rotation rate and the Snodgrass and Ulrich (1990) supergranule rotation rate are somewhat larger than the RLS rotation rates at all depths at the equator.

Figure 9 shows essentially the same curves as Figure 8, with the Snodgrass and Ulrich (1990) supergranulation rotation subtracted from each of the other curves. The differences in rotation rates is clearer. At ± 20 degrees there is a difference of 5 nHz between the supergranulation rotation rate and the plasma above 0.95 $R_\odot$. By mid-latitudes these differences are not as large. At latitudes (≥ 60) the supergranulation rotation rate falls below that of the plasma at depths below 0.97 $R_\odot$.

4. Conclusions

A realistic model of supergranulation must explain the existence of zonal flows, the m dependence, and the high rates of rotation.

4.1. Zonal Flows

The zonal flows (also known as torsional oscillations) illustrated in Figures 6 and 7 are quite interesting. Supergranule rotation is affected locally by mean flows. The agreement with the overlapping f-mode results is impressive, in particular for the RLS inversion. It is worth noting that while the f-mode results have a resolution of $5 - 10^\circ$ the results presented here have a resolution of roughly 1° at the equator. Also, the present analysis is able to measure the anti-symmetric component of zonal flows, unlike the f-mode inversion analysis. The origin of the zonal flows is largely unknown, although some theories have been proposed. Hopefully accurate measurements such as these, and those from p and f modes will be able to guide the theoretical work. Other measurements and properties of the zonal flows are discussed in Schou *et al.* (1998), Schou (1999) and Toomre *et al.* (1999).

4.2. Size Does Matter

One of the most puzzling results of this analysis is the m dependence of the inferred rotation rate, as illustrated in Figure 4. It has been observed earlier that the supergranulation rotation rate, as measured by correlation tracking, depends on the time lag with longer time lags

giving higher rotation rates (Duvall, 1980). Assuming that the larger scale features dominate at large lags (for instance by having a longer lifetime) this is consistent with the results shown here. The Snodgrass and Ulrich (1990) rotation rate shown here was measured using images binned to 34×34 pixels corresponding to a Nyquist m value of 50 at the equator, which is indeed roughly the size scale where that measurement agrees with the one presented here.

The m dependence of rotation may be due to two phenomena with size-dependent visibility and different rotation rates. The less rapidly rotating one would dominate at high-m and the more rapid rate would dominate at low-m. The difference in rotation rates in Figure 4 is comparable to the FWHM of the peak in Figure 3 so there may be two ridges which the current analysis cannot resolve. The rotation at $m = 30$ is $\approx 6\%$ faster than the maximum rotation rate from the RLS inversions of Schou *et al.* (1998), indicating that the faster phenomena would not be due to simple convection.

4.3. Super-Rotating Supergranules

The simple model of supergranules as convection cells anchored at a characteristic depth does not fit. Supergranules rotate faster than the plasma at their estimated anchor depth. Either supergranules are rooted much deeper than predicted or they rotate faster than the surrounding plasma.

One explanation is that supergranules are not a purely convective phenomenon. Supposing that waves play a role in the formation of supergranules and the waves propagate in a prograde direction, the supergranules could appear to be rotating faster than the solar plasma. Wolff (1996, 1995) suggested that r modes could modulate convection at the base of the H and He ionization zones where the convection is strengthened (at a depth of $0.932\ R_\odot$), where r modes have high viscous energy loss. Notably, this depth most closely matches the supergranule rotation rate near the equator. Further, an interesting property of r modes is that the propagation speed depends on the degree, l, and order, m, of the mode. This dependency could also explain the supergranulation rotation dependency of m.

Acknowledgements

SOHO is a project of international cooperation between ESA and NASA. This research is supported by the SOI-MDI NASA grant NAG5-3077 at Stanford University.

References

Beck, J.G., Duvall, T.L. Jr. and Scherrer, P.H.: 1998, *Nature*, **394**, 653.

Beckers, J.M: 1968, *Solar Phys*, **5**, 309.

Duvall, T.L., Jr.: 1980, *Solar Phys.* **66**, 213.

Duvall, T.L., Jr.: 1998, in S. Korzennik and A. Wilson (eds.) *Structure and Dynamics of the Interior of the Sun and Sun-like Stars*, **SP-418**, 581.

Duvall, T.L., Jr, Kosovichev, A.G., Scherrer, P.H., Bogart, R.S., Bush, R.I., De Forest, C., Hoeksema, J.T., Schou, J., Saba, J.L.R., Tarbell, T.D., Title, A.M., Wolfson, C.J. and Milford, P.N.: 1997, *Solar Physics*, **170**, 63.

Foukal, P. and Fowler, L.: 1984, *Astrophys. J.*, **281**, 442.

Hathaway, D.H.: 1988, *Solar Phys.*, **117**, 1.

Hathaway, D.H., Gilman, P.A., Harvey, J.W., Hill, F., Howard, R.F., Jones, H.P., Kasher, J.C., Leibacher, J.W., Pintar, J.A. and Simon, G.W.: 1996, *Science*, **272**, 1306.

Leighton, R., Noyes, R., and Simon, G.: 1962, *Astrophys. J.*, **135**, 474.

Lin, H, and Kuhn, J.R.: 1992, *Solar Phys.*, **141**, 1.

Schou, J.: 1999, *Astrophys. J.*, **523**, L181.

Schou, J., Antia, H.M., Basu, S., Bogart, R.S., Bush, R.I., Chitre, S.M., Christensen-Dalsgaard, J., Di Mauro, M.P., Dziembowksi, W.A., Eff-Darwich, A., Gough, D.O., Haber, D.A., Hoeksema, J.T., Howe, R., Korzennik, S.G., Kosovichev, A.G., Larsen, R.M., Pijpers, F.P., Scherrer, P.H., Sekii, T., Tarbell, T.D., Title, A.M., Thompson, M.J. and Toomre, J.: 1998 *Astrophys. J.* **505**, 390.

Simon, G. and Leighton, R, 1964, *Astrophys. J.*, **140**, 1120.

Snodgrass, H.B. and Ulrich, R.K.: 1990, *Astrophys. J.* **351**, 309.

Toomre, J., Christensen-Dalsgaard, J.C., Howe, R., Larsen, R.M., Schou, J., and Thompson, M.J.: 1999, *These Proceedings.*

Wolff, C.L.: 1995, *Astrophys. J.* **443**, 423.

Wolff, C.L.: 1996, *Astrophys. J. Letters* **459**, L103.

Worden, P.: 1975, *Solar Phys.*, **45**, 21.